

# Ultrametricity in the Edwards-Anderson Model

Pierluigi Contucci,<sup>1</sup> Cristian Giardinà,<sup>2</sup> Claudio Giberti,<sup>3</sup> Giorgio Parisi,<sup>4</sup> and Cecilia Vernia<sup>5</sup>

<sup>1</sup> *Università di Bologna, Piazza di Porta S. Donato 5, 40127 Bologna, Italy*

<sup>2</sup> *Eurandom, P.O. Box 513 - 5600 MB Eindhoven, The Netherlands*

<sup>3</sup> *Università di Modena e Reggio Emilia, via G. Amendola 2 -Pad. Morselli- 42100 Reggio Emilia, Italy*

<sup>4</sup> *Università La Sapienza di Roma, Roma, Italy*

<sup>5</sup> *Università di Modena e Reggio Emilia, via Campi 213/B, 41100 Modena, Italy*

We test the property of ultrametricity for the spin glass three-dimensional Edwards-Anderson model in zero magnetic field with numerical simulations up to  $20^3$  spins. We find an excellent agreement with the prediction of the mean field theory. Since ultrametricity is not compatible with a trivial structure of the overlap distribution our result contradicts the droplet theory.

Ὁ ἀναξ οὐ τὸ μαντεῖόν ἐστι τὸ ἐν Δελφοῖς  
οὔτε λέγει οὔτε κρύπτει ἀλλὰ σημαίνει  
*Heraclitus Fragment 93,*

from Plutarch, On the Pythian Oracle, 404E. [1]

Ultrametricity is a widely accepted property of the mean field spin glass theory: it is a crucial ingredient in the field theoretical computations of the Sherrington Kirkpatrick model [2–4] as well as a guiding principle for the rigorous proof of its free energy density formula [5, 6]. Its relevance in finite dimensional systems is nonetheless still an open matter, subject of intense investigations and debates in the theoretical and mathematical physics communities. Ultrametricity states a very striking property for a physical system: sampling three configurations independently with respect to their common Boltzmann-Gibbs state and averaging over the disorder, the distribution of the distances among them is supported, in the limit of very large systems, only on equilateral and isosceles triangles with no scalenus contribution. The relative weight of equilateral and isosceles triangles is then fixed by the so called *stochastic stability* property introduced for the infinite range spin glass model in [7, 8] and later proved also for the realistic short ranged models in finite dimensions [9, 10].

The property of ultrametricity and the non-trivial structure of the overlap distribution are the characterizing features of the mean field picture and are mutually intertwined: a trivial (delta-like) overlap distribution, like the one predicted in the droplet theory [11], is not compatible in fact with the previous ultrametric structure because it predicts only equilateral triangles.

In this letter we study the Edwards-Anderson model [12] for the spin glasses in the three-dimensional cubic lattice with  $\pm J$  random interactions (for a numerical study in four dimensions see [13]). With a multi-spin coding and a parallel-tempering algorithm we numerically investigate the distribution of overlaps for systems whose number of spins ranges from  $10^3$  to  $20^3$  at different temperatures. All the parameters used in the simulations are reported in Tab.I.

We find very strong indication in favor of ultrametricity which turns out to be reached at large volumes with exactly the form predicted by the mean field theory and, by consequence, a robust signal against droplet theory (for a study of dynamical ultrametricity and for the relation between statics and dynamics in spin glasses see [14, 15]).

From a mathematical point of view the triple  $(c_{1,2}, c_{2,3}, c_{31})$ , with  $0 \leq c_{i,j} \leq 1$ , representing the overlaps among three copies of the system, is called *stochastically stable and ultrametric* when, defining  $\chi(c) = \int_0^c P(c')dc'$ , its joint

$L$	Sweeps	Nreal	$n_\beta$	$T_{min}$	$T_{max}$
10	1047552	1280	25	0.7	2.1
12	1047552	896	25	0.7	2.1
16	1047552	704	25	0.7	2.1
18	2096128	768	49	0.7	2.1
20	2096128	512	103	0.7	2.1

Table I: Parameters of the simulations: system size, number of sweeps, number of disorder realizations, number of temperature values allowed in the parallel tempering procedure, minimum and maximum temperature values.

probability distribution function has the following structure:

$$\begin{aligned}
P(c_{1,2}, c_{2,3}, c_{3,1}) &= \frac{1}{2}P(c_{1,2})\chi(c_{1,2})\delta(c_{1,2} - c_{2,3})\delta(c_{2,3} - c_{3,1}) \\
&+ \frac{1}{2}P(c_{1,2})P(c_{2,3})\theta(c_{1,2} - c_{2,3})\delta(c_{2,3} - c_{3,1}) \\
&+ \frac{1}{2}P(c_{2,3})P(c_{3,1})\theta(c_{2,3} - c_{3,1})\delta(c_{3,1} - c_{1,2}) \\
&+ \frac{1}{2}P(c_{3,1})P(c_{1,2})\theta(c_{3,1} - c_{1,2})\delta(c_{1,2} - c_{2,3}) .
\end{aligned} \tag{1}$$

Thinking of the quantities  $c$ 's as 1 minus the sides of a triangle the previous formula says that only equilateral (first term on the right hand side of eq. (1)) and isosceles (last three terms of eq. (1)) triangles are allowed, the scalenus have zero probability. A standard computation allows to compute from (1) the distribution of the three random variables  $u = \min(c_{1,2}, c_{2,3}, c_{3,1})$ ,  $v = \text{med}(c_{1,2}, c_{2,3}, c_{3,1})$  and  $z = \max(c_{1,2}, c_{2,3}, c_{3,1})$  which turns out to be

$$\rho(u, v, z) = \frac{1}{2}x(u)P(u)\delta(v - u)\delta(z - v) + \frac{3}{2}P(z)P(v)\theta(z - v)\delta(v - u) , \tag{2}$$

and from that deduce the distribution of the two differences  $x = v - u$ ,  $y = z - v$

$$\tilde{\rho}(x, y) = \frac{1}{4}\delta(x)\delta(y) + \frac{3}{4}\int_y^1 2P(a)P(a - y)\theta(y)\delta(x)da , \tag{3}$$

whose marginals are

$$\tilde{\rho}(x) = \delta(x) , \tag{4}$$

$$\tilde{\rho}(y) = \frac{1}{4}\delta(y) + \frac{3}{4}\int_y^1 2P(a)P(a - y)\theta(y)da . \tag{5}$$

We recall that the Hamiltonian of the EA model [12] is given by

$$H_\sigma = - \sum_{|i-j|=1} J_{i,j}\sigma_i\sigma_j \tag{6}$$

with  $J_{i,j} = \pm 1$  symmetrically distributed and Ising spins  $\sigma_i$ . Given two spin configurations  $\sigma$  and  $\tau$  for a system of linear size  $L$ , we consider the main observables: the link-overlap

$$Q(\sigma, \tau) = (3L^3)^{-1} \sum_{|i-j|=1} \sigma_i\sigma_j\tau_i\tau_j \tag{7}$$

which is the normalized Hamiltonian covariance, and the standard overlap

$$q(\sigma, \tau) = (L^3)^{-1} \sum_i \sigma_i\tau_i \tag{8}$$

which is related to the Edwards-Anderson order parameter. For every function of two spin configurations  $c(\sigma, \tau)$  (for instance  $Q$  or  $q$ ) the physical model induces a probability distribution by the formula

$$\mathcal{P}(c_{1,2}, c_{2,3}, c_{3,1}) = \text{Av} \left( \frac{\sum_{\sigma, \tau, \gamma} \delta(c_{1,2} - c(\sigma, \tau))\delta(c_{2,3} - c(\tau, \gamma))\delta(c_{3,1} - c(\gamma, \sigma)) \exp -\beta[H_\sigma + H_\tau + H_\gamma]}{\sum_{\sigma, \tau, \gamma} \exp -\beta[H_\sigma + H_\tau + H_\gamma]} \right) , \tag{9}$$

where Av represents the average over the disorder  $J_{i,j}$ . In the sequel the brackets  $\langle - \rangle$  will denote the average with respect to distribution (9).

We find very strong evidences that for large volumes the link overlap has the ultrametric structure of eq. (1). Since the standard overlap instead has a symmetric distribution in the interval  $[-1, 1]$  we find that formula (1) is verified up to a global gauge transformation (see details below).

The results can be described as follows. We test numerically the structure of the distribution for the two random variables  $X = Q_{med} - Q_{min}$  and  $Y = Q_{max} - Q_{med}$  where the  $Q$ 's represent the largest, medium, and smaller value of the link-overlap among three copies of the system.

The numerical data are compared to the formulas (4) and (5) both from the point of view of the first and second moment and also for the whole distribution.

- Figure 1: The two panels show the plot of  $\langle X \rangle / \langle Q \rangle$  (left) and  $\langle Y \rangle / \langle Q \rangle$  (right) as functions of the temperature  $T$ . We see that the average value of the  $X$  variable is much closer to zero than that of the  $Y$  variable. Nevertheless both averaged variables show some tendency toward zero. Since ultrametricity implies that the first quantity goes to zero while the other doesn't we perform the analysis of the second moments and of the distributions in order to resolve the behavior of the two variables.
- Figure 2: We find that the variances of the two variables have a totally different behavior. The left panel contains the plot of  $Var(X)/Var(Q)$  and the right panel of  $Var(Y)/Var(Q)$  both as a function of  $Var(Q)$ . We find more convenient this parametrization with respect to the usual one using temperature because it allows to extract more information on size dependence through scaling laws: this is due to the fact that both  $Var(Y)$  and  $Var(Q)$  have size dependence changing with  $T$ . In particular within the temperature range that we have taken into account the quantity  $Var(Q)$  decreases monotonically with the temperature. The figure clearly shows that while the variance of  $X$  is shrinking to zero the variance of  $Y$  is growing with the volume. Moreover the variance of  $X$  satisfy a scaling law with very good accuracy:  $Var(X)/Var(Q)$  scales like  $L^{-1.17}$  (see inset) while there is no scaling law for the second variable.
- Figure 3: The figure displays for two system sizes of  $L = 12$  and  $L = 20$  the data histograms for  $X$  (in black) and  $Y$  (in red) variable at  $T = 0.7$ . They show that  $P(X)$  is much more concentrated close to zero, while  $P(Y)$  is spread on a larger scale. The function  $\rho(Y)$  provides a test of consistency with formula (5). The plot of  $\rho(Y)$  has been obtained using the data histograms for the function of  $X$  to represent the delta function (4) and the experimental data for the distribution of  $Q$  inside the convolution. The two curves superimpose each other with an excellent agreement. We have also tested that any different numerical weight other than  $1/4$  and  $3/4$  do not yield such an agreement.

The previous results clearly show that the link overlap has an ultrametric distribution. Our next investigation is about the standard overlap for which we claim that it also obeys ultrametricity. Given the three standard overlaps  $q_{1,2}, q_{2,3}, q_{1,3}$  their probability measure is a priori supported on  $[-1, 1]^3$ . Gauge invariance ( $q_{i,j} \rightarrow \alpha_i q_{i,j} \alpha_j$ , with  $\alpha = \pm 1$ ) implies that it is a sum of two gauge orbits, one for  $S = \text{sign}(q_{1,2}q_{2,3}q_{1,3}) > 0$  and the other for  $S < 0$ . To investigate the contribution of the frustrated couples ( $S < 0$ ) we plotted the quantity (see tilded  $q$ 's below)  $S^{(-)} = \int_{-1}^0 d\tilde{q}_{1,3} p(\tilde{q}_{1,3}) \tilde{q}_{1,3}^2 / \int_{-1}^1 d\tilde{q}_{1,3} p(\tilde{q}_{1,3}) \tilde{q}_{1,3}^2$ : the left panel of Fig. 4 clearly show that the distribution of  $\tilde{q}_{1,3}$  is supported almost completely on the positive interval and that the negative values are concentrated near zero (for similar quantities and also three-replicas observables see [16]). This implies that the contribution associated to the frustrated orbit ( $S < 0$ ) is very small at large volumes. These results can be summarized saying that the distribution of the  $q$  is given by

$$\begin{aligned} \bar{P}(q_{1,2}, q_{2,3}, q_{3,1}) = & \frac{1}{4} [P(q_{1,2}, q_{2,3}, q_{3,1})\theta(q_{1,2})\theta(q_{2,3})\theta(q_{3,1}) + P(-q_{1,2}, -q_{2,3}, q_{3,1})\theta(-q_{1,2})\theta(-q_{2,3})\theta(q_{3,1}) \\ & + P(q_{1,2}, -q_{2,3}, -q_{3,1})\theta(q_{1,2})\theta(-q_{2,3})\theta(-q_{3,1}) + P(-q_{1,2}, q_{2,3}, -q_{3,1})\theta(-q_{1,2})\theta(q_{2,3})\theta(-q_{3,1})] \end{aligned} \quad (10)$$

and that to check ultrametricity for the standard overlap is equivalent to check that the  $P$  appearing on the right hand side of (10) is given by (1). Equivalently that can be done defining the new random variables

$$\tilde{q}_{1,2} = \max(|q_{1,2}|, |q_{2,3}|, |q_{1,3}|) \quad (11)$$

$$\tilde{q}_{2,3} = \text{med}(|q_{1,2}|, |q_{2,3}|, |q_{1,3}|) \quad (12)$$

$$\tilde{q}_{1,3} = \text{sign}(q_{1,2}q_{2,3}q_{1,3}) \min(|q_{1,2}|, |q_{2,3}|, |q_{1,3}|) \quad (13)$$

and checking that they obey distribution (1). We have made simulation on those random variables and found results (not shown for the sake of space) in total agreement with ultrametricity as those for the link overlap. This indeed extends previous findings of [17, 18] where it was shown that link and standard overlaps are mutually non fluctuating for the case of Gaussian coupling. In the right panel of Fig. 4 we show for the model with  $\pm J$  investigated within this work the analysis of the realtive fluctuation and functional dependence of the two overlaps. It is shown the function  $G(q^2) = \langle Q|q^2 \rangle$ , i.e. the expected value of the link-overlap for an assigned value of the standard overlap, for different system sizes at  $T = 0.7$ , with a fit to the infinite volume limit  $g_\infty(q^2)$ . The conditional variance of  $Q$  given  $q^2$ , displayed in the inset, shows a trend toward a vanishing variance for infinite system sizes.

Numerical simulations, like the Delphi Oracle for Heraclitus, neither conceal or reveal the truth, but only hint at it. In this work we have investigated the property of ultrametricity in a short-range spin-glass model. We have shown that violations of ultrametricity in finite volumes have a clear tendency to vanish as the system size increases. We verified moreover that the analytical predictions of the ultrametric replica symmetry breaking ansatz are correct up to the tested sizes. Our results contradicts previous finding [19] done for much smaller volumes (up to  $8^3$ ) in which lack of ultrametricity was claimed. We have shown instead strong numerical evidence that the spin glass in three dimensions fulfills the property of ultrametricity for both the link and the standard overlap distributions. A detailed account of the present investigation will appear elsewhere [20].

**Acknowledgments.** We thank S. Graffi, F. Guerra, E. Marinari, C. Newman, D. Stein and F. Zuliani for useful discussions. C. Giardinà and C. Vernia acknowledge GNFM-INdAM for financial support.

- 
- [1] G.S.Kirk, J.E.Raven,M.Schofield., *The Presocratic Philosophers* Cambridge University Press (1995)
  - [2] D. Sherrington and S. Kirkpatrick, *Phys. Rev. Lett.* **35**, 1792 (1975).
  - [3] M. Mezard, G. Parisi, M.A. Virasoro, *Spin Glass Theory and Beyond* World Scientific, Singapore (1987).
  - [4] G. Parisi, F. Ricci-Tersenghi, *J. Phys. A: Math. Gen.* **33**, 113, (2000).
  - [5] F. Guerra, *Comm. Math. Phys.* **233**, 1, (2003).
  - [6] M. Talagrand, *Annals of Math.* **163**, 221 (2006). This result is announced in *C.R.A.S.* **337**, 111, (2003).
  - [7] M. Aizenman, P. Contucci *J. Stat. Phys.* **92**, 765, (1998).
  - [8] F. Guerra, *Int. Jou. Phys. B* **10**, 1675, (1997).
  - [9] P. Contucci, *J. Phys. A: Math. Gen.* **36**, 10961, (2003).
  - [10] P. Contucci, C. Giardinà, *Jour. Stat. Phys.* to appear (2006). *math-ph/0505055*
  - [11] D.S. Fisher and D.A. Huse, *Phys. Rev. Lett.* **56**, 1601 (1986)
  - [12] S.F. Edwards and P.W. Anderson, *Jou. Phys. F.*, **5**, 965, (1975).
  - [13] A. Cacciuto, E. Marinari, G. Parisi *J. Phys. A: Math. Gen* **30** L263-L269 (1997)
  - [14] S. Franz, F. Ricci-Tersenghi *Phys. Rev. E* **61**, 1121-1124 (2000)
  - [15] S. Franz, M.Mezard, G.Parisi, L.Peliti *Phys. Rev. Lett.* **81**, 1758 (1998)
  - [16] D. Iñiguez, G. Parisi, J. Ruiz-Lorenzo *J. Phys. A: Math. Gen.* **29** 4337-4345 (1996)
  - [17] P. Contucci, C. Giardinà, C. Giberti, C. Vernia *Phys. Rev. Lett.* **96**, 217204 (2006)
  - [18] E. Marinari, G. Parisi *Phys. Rev. Lett.* **86**, 3887-3890 (2001)
  - [19] G. Hed, A. P. Young, E. Domany *Phys. Rev. Lett.* **92**, 157201 (2004)
  - [20] P. Contucci, C. Giardinà, C. Giberti, G. Parisi, C. Vernia, in preparation.

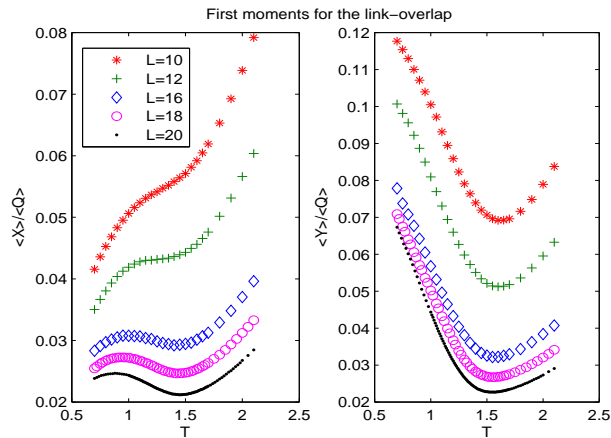


Figure 1: Normalized first moments of the two random variables  $X = Q_{med} - Q_{min}$  and  $Y = Q_{max} - Q_{med}$ .

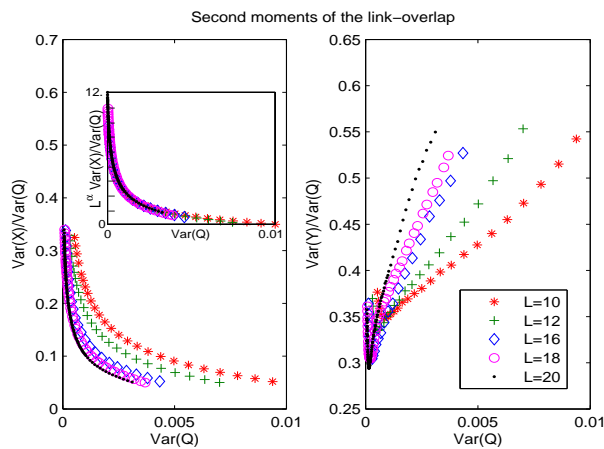


Figure 2: Normalized variances of the two random variables  $X = Q_{med} - Q_{min}$  (left) and  $Y = Q_{max} - Q_{med}$  (right). The inset (at left) shows the scaling law for  $\alpha = 1.17$ , i.e.  $L^\alpha Var(X)/Var(Q)$  is  $L$ -independent.

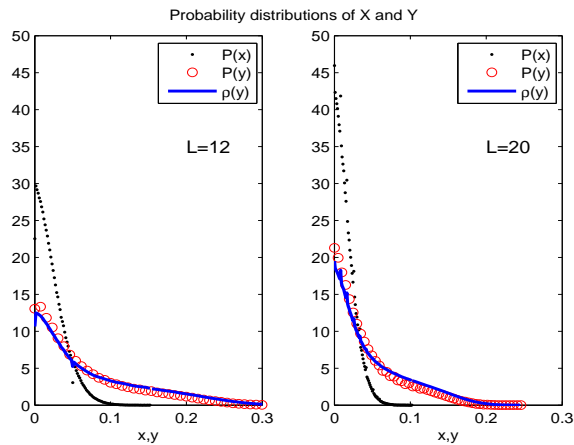


Figure 3: Histograms for  $X = Q_{med} - Q_{min}$  and  $Y = Q_{max} - Q_{med}$  for the two system sizes ( $L = 12$  and  $L = 20$ ) at temperature  $T = 0.7$ .  $\rho(Y)$  shows the distribution of  $Y$  computed from formula (5) using experimental data for  $P(Q)$  and approximating the delta function with the histogram of  $X$

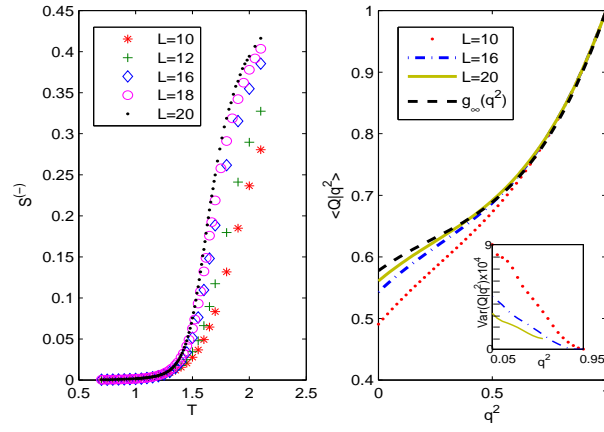


Figure 4: Left panel: the average value of  $S^{(-)}$  (defined before Eq. (10) in the text) as a function of  $T$ . Right panel: Conditional expectation and conditional variance (inset) of the random variable  $Q$  given  $q^2$ , where  $Q$  is the link-overlap and  $q^2$  is the square of the standard overlap, for different system sizes at temperature  $T = 0.7$